

## EVALUATION OF THE DESTRUCTION POTENTIAL OF Zr-DOPED TiO<sub>2</sub> NANOPARTICLES FOR THE ABATEMENT OF H<sub>2</sub>S GAS

N. SHAHZAD<sup>a,\*</sup>, N. ALI<sup>b</sup>, N. AHMAD<sup>c</sup>

<sup>a</sup>National University of Sciences and Technology (NUST), 44000, Pakistan

<sup>b</sup>Government Post graduate Jahanzeb College Saidu Sharif Swat, 19130, Pakistan,

<sup>c</sup>Nanoscience and Catalysis Division, National Centre for Physics, QAU Campus, Islamabad, 43520, Pakistan.

Due to its toxicity, destruction of H<sub>2</sub>S gas has been an important topic of researchers. Many studies have been carried for investigating various techniques for the removal of this gas. One of those techniques is catalytic and photocatalytic destruction of H<sub>2</sub>S gas using various catalysts including TiO<sub>2</sub> owing to its significant potential for degradation of various pollutants. This study investigates the destruction potential of Zr doped TiO<sub>2</sub> for the abatement of H<sub>2</sub>S gas. The catalysts were characterized using different techniques like XRD, SEM, XRF. The catalytic experiments were performed using fixed bed catalyst system. The samples were analyzed using GC-MC technique and it was revealed that the Zr doping of TiO<sub>2</sub> did not favour positively towards enhancing the H<sub>2</sub>S destruction potential as found in other studies.

(Received May 14, 2020; Accepted September 14, 2020)

*Keywords:* TiO<sub>2</sub>, H<sub>2</sub>S, Catalytic, Destruction, Potential

### 1. Introduction

In addition to primary pollutants like NO<sub>x</sub> and SO<sub>x</sub>, there are a lot of pollutants that need attention, and one of them is H<sub>2</sub>S gas. It has become an environmental concern due to its peculiar rotten egg smell and lower odour threshold [1]. This gas has been found to be highly toxic, flammable and malodorous and since it is heavier than air, it gets accumulated in poorly ventilated spaces [2]. H<sub>2</sub>S gas is emitted into the atmosphere by different sources, out of which approximately 90 percent are natural [3], which include decomposition of dead plant and animal material, especially when this occurs in wet conditions with limited oxygen, hot springs, volcanoes, and other geothermal sources. Anthropogenic sources include industrial processes, primarily from the petrochemical and natural gas extraction and refining processes and from manufacturing industries of paper and pulp. It has been found in many research studies that 90% of the H<sub>2</sub>S is found in the coal-derived gaseous products containing sulfur [4]. In addition to this, manure-handling plants, sewage treatment plants, coke oven plants and tanneries, also contribute to the H<sub>2</sub>S gas emission into the air [3]. H<sub>2</sub>S gas is considered to be a broad spectrum toxicant as it is highly toxic for humans [5]. Because of it being colourless, it can be inhaled and directly affect the nervous system leading to adverse affects on humans. Human exposures to high concentrations of about 2000 ppm may result in breathing difficulties and ultimately death may occur within a very short span of time [6].

Lot of techniques and methods are being followed throughout the world for removal or reducing H<sub>2</sub>S gas emissions to permissible or desirable levels including, Claus process, LO-CAT process, Pure and mixed metal oxide sorbets and so on. Photocatalysis has also been used for carrying out gas phase destruction of toxic volatile compounds, including H<sub>2</sub>S gas using TiO<sub>2</sub> catalyst under UV/Visible light conditions [7]. Furthermore, many metal and non metal dopants have also been used to enhance the H<sub>2</sub>S destruction potential of TiO<sub>2</sub> nanomaterials [8-11]. In our previous studies, we used sulphur doped TiO<sub>2</sub> nanomaterials for the destruction of H<sub>2</sub>S gas [12-

---

\* Corresponding author: naeemshahzad@mce.nust.edu.pk

14]To further the explore the  $\text{TiO}_2$  destruction potential of  $\text{H}_2\text{S}$  gas, we changed the dopant and used Zr for this purpose. Since, Zr has been found to improve the thermal stabilization of  $\text{TiO}_2$  and it also increases its surface area [15, 16]. In another study, the photocatalytic decomposition efficiency of Zr-doped  $\text{TiO}_2$  films, measured with stearic acid coating was increased by 50% as compared to undoped  $\text{TiO}_2$  films[17].

In this study we have used Zr doped  $\text{TiO}_2$  nanoparticles and compared its destruction potential with our previous results using sulphur doped nanomaterials to assess the  $\text{H}_2\text{S}$  destruction efficiency of Zr doped  $\text{TiO}_2$  nanoparticles.

## 2. Materials and methods

### 2.1. Materials

All reagents used were of analytical grade. All the solutions were prepared in distilled water (E.C.  $2.8\mu\text{S}/\text{cm}$ ) which was obtained from the distillation apparatus (Model WSB/4, Hamilton Laboratory Glass Ltd.).  $\text{ZrOCl}_2 \cdot 8\text{H}_2\text{O}$  (Merck), precursor was used for doping  $\text{TiO}_2$  nanoparticles with Zr.  $\text{H}_2\text{S}$  (8%) and Ar gas procured from BOC specialist gases Ltd, UK were used in the experiment.

### 2.2. Synthesis of Zr doped $\text{TiO}_2$ nanoparticles

Zirconium (Zr) doped  $\text{TiO}_2$  nanoparticles were synthesized using co-precipitation method [18] with slight modification. The weight of Zr salt required to achieve corresponding Zr dopant percentage in the nanoparticles was calculated by molar ratios. Zr doped  $\text{TiO}_2$  nanoparticles were prepared by adding required amount of Zirconium Chlorated solution into the  $\text{TiO}_2$  suspension and the solution was titrated with 3M NaOH till pH reached 4. The precipitates were collected, washed with distilled water, dried at  $105^\circ\text{C}$ , overnight and calcined at  $500^\circ\text{C}$  for 6 hrs to get Zr-doped  $\text{TiO}_2$  nanoparticles.

### 2.3. Characterization

Characterization was carried out using the same techniques, XRD, XRF and SEM, as used in our study for S-doped  $\text{TiO}_2$  nanoparticles[12].

### 2.4. Experimental design

The experiments were conducted using pure and Zr-doped  $\text{TiO}_2$  nanoparticles. For the purpose of identification they were given different codes. The amples after the experiments (spent samples) were identified by adding the letter ‘S’ after their respective codes, which have been tabulated in Table 1.

Table 1. Sample identification codes for nanoparticles.

Sr no.	Sample	Sample code
1.	Pure $\text{TiO}_2$ nanoparticles	0P
2.	Pure $\text{TiO}_2$ nanoparticles (spent)	0PS
3.	1% Zr-doped $\text{TiO}_2$ nanoparticles	1ZrP
4.	1% Zr-doped $\text{TiO}_2$ nanoparticles (spent)	1ZrPS
5.	2% Zr-doped $\text{TiO}_2$ nanoparticles	2ZrP
16.	2% Zr-doped $\text{TiO}_2$ nanoparticles (spent)	2ZrPS

## 2.5. Catalytic reactions

Fixed bed catalysis system was used to carry out experiments for evaluating the net destruction of H<sub>2</sub>S gas. The experimental arrangement is shown in Figure 1, which are similar to another study conducted by our group for S-doped TiO<sub>2</sub> nanoparticles[7]. Before running the experiment, the whole system was flushed with Ar gas to remove any residuals in the system. 0.1 gm of the catalyst was loaded in the centre of the glass tube with quartz wool at both ends. This tube was placed in the centre of the furnace along with the thermocouple to control the temperature. All the experiments were carried out at 450°C because it was noted from another study that H<sub>2</sub>S removal efficiency of ZnO was found to be maximum at this temperature and it was reduced with further increase in temperature[19].

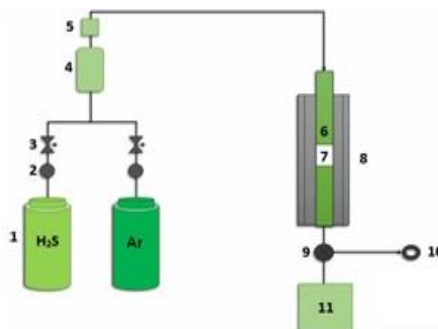


Fig.1. Fixed Bed Catalyst System used for the catalytic gas phase destruction of H<sub>2</sub>S gas using TiO<sub>2</sub> nanoparticles (1-Gas Cylinders, 2-Gas flow controllers, 3-Flow Meters, 4-Greaseless stopcocks, 5-Wash Bottles, 6-Glass Tube, 7-Loaded sample, 8-Furnace, 9-Multi flow controller, 10- Gas sampling port, 11-Exhaust).

H<sub>2</sub>S gas cylinder was then connected to this system and the gas was passed through this setup. 1<sup>st</sup> gas sample was collected from the gas sampling port immediately, to be used as reference. The temperature of the furnace was raised to 450°C gradually. At this temperature, 3 samples were taken after interval of 1 hr and analyzed by GC-MS. The net reduction in the H<sub>2</sub>S gas peak areas was calculated by difference in the peak areas of the reference and other samples.

## 2.6. H<sub>2</sub>S gas analysis

The H<sub>2</sub>S gas analysis was carried out by using the Gas-Chromatography-Mass Spectroscopy (GC-MS) using Shimadzu QP-5050 using DB5-MS (J and W Scientific) 30m, id 0.25mm and film thickness of 0.25µm, for the gas samples collected after the catalytic experiments. The GC-MS analysis was done

## 3. Results and discussions

### 3.1. Physical properties

#### 3.1.1. XRD spectra

The pure and Zr doped TiO<sub>2</sub> nanoparticles were characterized using XRD and corresponding spectra of the samples before and after the experiments are shown in Figures 2 and 3. By observing the XRD spectra of all the samples before the experiment correspond to anatase phase since almost all the peaks of all the samples match the peaks of anatase phase as confirmed by JCPDS standard files no. 21-1272. The average crystallite sizes of the nanoparticles were calculated from the most intense diffraction peak using the Scherrer's Equation and is as shown in Table 2.

Table 2. Crystallite sizes of pure and doped TiO<sub>2</sub> nanoparticles calculated from the Scherrer's equation.

Sample ID	B (radians)	2θ (degrees)	Diameter (nm)
0P	0.0164	25.4331	8.2
1ZrP	0.0082	25.4092	16.3
2ZrP	0.0093	25.4117	14.5

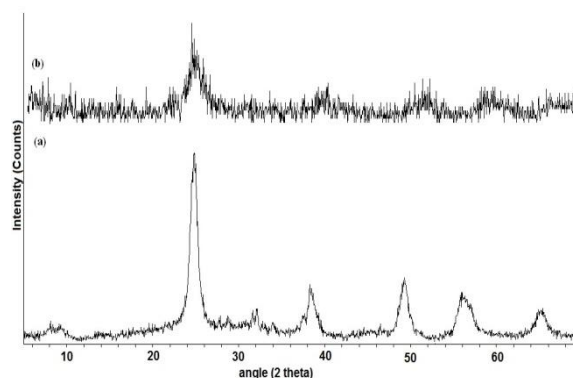


Fig.2. XRD spectrum of 1ZrP (a) before the experiment, (b) spent sample.

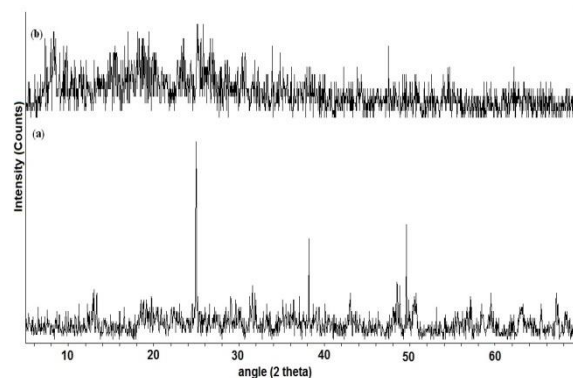


Fig.3. XRD spectrum of 2ZrP (a) before the experiment, (b) spent sample.

By observing the spectra in Figure 2 (a) and 3 (a), it was found that the major peaks recorded at  $2\theta$  have been correspond to the crystalline anatase phase of TiO<sub>2</sub>. However, the spent samples show a lot of noise which is a consequent of reactions during the experiments at a high temperature of 450°C [7].

### 3.1.2. SEM analysis

SEM micrographs analysis of pure and Zr doped TiO<sub>2</sub> nanoparticles before and after the experiments showed slight change as the amount of sulfur adsorbed on the TiO<sub>2</sub> surface of the spent samples including pure and Zr-doped TiO<sub>2</sub> nanoparticles was not very significant and could have been further investigated using TEM since in one of the study, a close analysis using TEM showed that the TiO<sub>2</sub> nanoparticles were made up of loosely and aggregated nanoparticles which can also be observed in the SEM images of our samples [20].

### 3.1.3. XRF analysis

Energy Dispersive XRF was performed for all the nanoparticles before (fresh samples) and after the experiments (spent samples). The rest of the results of the samples have been tabulated in Table 3.

Table 3. Quantitative elemental analysis of TiO<sub>2</sub> nanoparticles.

Sample ID	Titanium (Ti)		Zirconium (Zr)		
	Mass %	Mol %	Mass %	Mol %	% Increase
<b>0P</b>	100	100	-	-	
<b>0PS</b>	99.09	99.23	0.91	0.77	<b>0.91</b>
<b>1ZrP</b>	98.81	99.32	1.19*Zr	0.68*Zr	
<b>1ZrPS</b>	98.03	98.53	1.19*Zr & 0.78*S	0.68*Zr	<b>0.78</b>
<b>2ZrP</b>	97.83	98.63	2.17*Zr	1.37*Zr	
<b>2ZrPS</b>	97.33	98.12	2.17*Zr & 0.5*S	1.37*Zr	<b>0.5</b>

As it was not possible to be very precise in dopant concentrations, the percentage dopant concentrations were considered after rounding it off to the nearest percentage, as 0.96% Zr concentration on TiO<sub>2</sub> nanoparticles have been taken as 1% Zr-doped TiO<sub>2</sub> nanoparticles for carrying out these experiments and similarly of 2% Zr-doped TiO<sub>2</sub> nanoparticles. The S adsorption on the Zr-doped TiO<sub>2</sub> nanoparticles was quite low ranging from 0.5-0.8% only and showing that S was not favourably being adsorbed on the surface of the Zr-doped TiO<sub>2</sub> nanoparticles and it was therefore likely that the H<sub>2</sub>S destruction efficiency was not going to be quite noticeable in this case.

### 3.1.4. GC MS analysis

All the gas samples obtained from the experiments were analyzed using GC-MS. The net reduction in the H<sub>2</sub>S gas peak areas was calculated by difference in the peak areas of the reference samples and the samples collected after an interval of one hour. Three samples were collected in all the experiments.

The results of the GC-MS analysis show that the highest reduction in concentrations of H<sub>2</sub>S gas after 3 hours of the experiments, have been observed for the TiO<sub>2</sub> nanoparticles doped with 2% Sulfur, in one of our study [7]. The destruction efficiency achieved after three hours of the experiment using Zr-doped TiO<sub>2</sub> nanoparticles was quite less as compared to TiO<sub>2</sub>nanoparticles which were found to be quite significant (91.71%). Despite the fact that they were still a bit lesser than observed by Canela et al. [21] in which they achieved 97% degradation using photocatalysis instead of high temperature catalysis used in this case. The GC-MS results are tabulated in Table 4.

Table 4. Percentage reduction in gas peak areas along with the degradation rates calculated using GC-MS analysis.

Sample ID	1 <sup>st</sup> Sample (60 mins) % Reduction	2 <sup>nd</sup> Sample (120 mins) % Reduction	3 <sup>rd</sup> Sample (180 mins) % Reduction
<b>0P</b>	26.3	60.07	91.71
<b>1ZrP</b>	17.8	19.71	27.11
<b>2ZrP</b>	1.68	2.64	17.36

In continuation of our other studies [7, 8, 13, 14] H<sub>2</sub>S destruction efficiency was assessed owing to the findings of another study in which authors observed 50% increase in photocatalytic activity when TiO<sub>2</sub> was doped with Zr [17]. The reason could be the same as stated for pure

TiO<sub>2</sub> nanoparticles above, but in this case the experimental conditions significantly affected the H<sub>2</sub>S destruction efficiency after doping TiO<sub>2</sub> with Zr. The results show that Zr doping does not prove to be favourable for H<sub>2</sub>S destruction, because in this case, the efficiency reduced considerably as compared to TiO<sub>2</sub> nanoparticles which were pure.

#### 4. Conclusions

The catalytic gas-phase destruction of H<sub>2</sub>S gas was studied using Zr-doped TiO<sub>2</sub> nanoparticles at 450°C. It was observed that H<sub>2</sub>S destruction was not positively favoured in this study at higher temperatures when doped with Zr, as observed for photocatalytic experiments in another study cited above. Pure TiO<sub>2</sub> nanoparticles showed significantly higher degradation potential for H<sub>2</sub>S gas than the nanoparticles after Zirconium doping. Further studies need to be carried out by varying the concentration of Zr-doping on nanoparticles and evaluating its effects on H<sub>2</sub>S destruction. These experiments also need to be repeated under different temperatures in order to find out the highest degradation efficiency at a particular temperature. In addition to this, further experiments need to be conducted in order to ascertain the induction time required for getting maximum reduction in the gas samples, which in this study was found to be 3 hours.

#### References

- [1] B. Mills, *Filtr. Separat.***32**(2),147 (1995).
- [2] Z. Shareefdeen, A. Aidan, W. Ahmed, M. B. Khatri, M. Islam, R. Lecheheb, F. Shams, *Int. J. Chem. Molec.***4**(2), 145 (2010).
- [3] L. Skrtic, MS thesis, University of California, Berkeley, USA, 2006.
- [4] T. H. Soerawidjaja, Ph.D. thesis, Delft University, Holland, 1985.
- [5] M. S. Legator, C. R. Singleton, D. L. Morris, D. L. Philips, *Arch. Environ. Health***56**(2), 123 (2001).
- [6] M. Tomar, T. H. A. Abdullah, *Water Res.***28**(12),2545 (1994).
- [7] N. Shahzad, S. T. Hussain, A. Siddiqua, M. A. Baig, *J. Nanosci. Nanotechno.***12**(6), 5061 (2012).
- [8] N. Shahzad, Q. Chen, *Mater. Sci. Forum* **756**,225 (2013).
- [9] H. Zhao, H. Yu, X. Quan, S. Chen, Y. Zhang, H. Zhao, H. Wang, *Appl. Catal. B-Environ.* **152–153**,46 (2014).
- [10] W. Zhao, W. Ma, C. Chen, J. Zhao, Z. Shuai, *J. Am. Chem. Soc.***126**(15),4782 (2004).
- [11] W. Choi, A. Termin, M. R. Hoffmann, *The J. Phys. Chem.***98**(51),13669 (1994).
- [12] N. Shahzad, Ph.D. thesis, National University of Sciences and Technology, Pakistan, 2012.
- [13] N. Shahzad, S. T. Hussain, N. Ahmad, *Chalcogenide Lett.* **10**(1), 19 (2013).
- [14] N. Shahzad, N. Ahmad, *Chalcogenide Lett.***12**,129 (2015).
- [15] G. Tian, K. Pan, H. Fu, L. Jing, W. Zhou, *J. Hazard. Mater.***166**(2),939 (2009).
- [16] B. Neppolian, Q. Wang, H. Yamashita, H. Choi, *Appl. Catal. A-Gen.***333**(2),264 (2007).
- [17] S. H. Qiu, T. L. Starr., *J. Electrochem. Soc.***154**(6),H472 (2007).
- [18] S. T. Hussain, K. Khan, R. Hussain, *J. Nat. Gas Chem.***18**(4),383 (2009).
- [19] H. Li, MS thesis, University of Pittsburgh, USA, 2008.
- [20] S. K. Choi, S. Kim, S. K. Lim, H. Park, *The J. Phys. Chem. C.***114**(39),16475 (2010).
- [21] M. C. Canela, R. M. Alberici, W. F. Jardim, *J. Photoch. Photobio. A.***112**(1),73 (1998).